



Research article

Piperine-hydroxybenzoate as phytochemistry antiosteoarthritis combination: Structural, solubility, and in vivo antiinflammatory study

Ari Sartinah^{a,c}, Hidehiro Uekusa^d, Yuto Abekura^d, Slamet Ibrahim^e,
Kusnandar Anggadiredja^a, Ilma Nugrahani^{a,b,*}

^a School of Pharmacy, Bandung Institute of Technology, Bandung 40132, Indonesia

^b Center of Halal Studies, Bandung Institute of Technology, Bandung 40132, Indonesia

^c Faculty of Pharmacy, Halu Oleo University, Kendari 93231, Indonesia

^d School of Science, Tokyo Institute of Technology, Tokyo 152-8551, Japan

^e Faculty of Pharmacy, Jenderal Achmad Yani University, Cimahi 40531, Indonesia

ARTICLE INFO

Keywords:

Solid-phase multicomponent
Piperine
4-Hydroxybenzoic acid
Piperine-hydroxybenzoate
Antiosteoarthritis

ABSTRACT

This study discusses the composition and structure determination of a new multicomponent system from antiinflammatory natural ingredients, consisting of piperine (Pip) and 4-hydroxybenzoic acid (HBA), named Pip-HBA. In addition, this research studied its solubility and anti-inflammatory activity. After screening the stoichiometric proportions, this multicomponent system formation reaction was carried out using the solvent-dropped grinding and evaporation methods. Characterizations using solid analysis including differential scanning calorimetry (DSC), powder X-ray diffractometry (PXRD), and Fourier transform infrared spectroscopy (FTIR), confirmed the formation of Pip-HBA. These multicomponent systems showed different thermograms and diffractograms. Furthermore, the FTIR spectrum of Pip-HBA multicomponent system differs from the physical mixture and its constituent components. Single crystal diffractometry (SCXRD) determined Pip-HBA to be a new multicomponent system structure in three dimensions. Pip-HBA showed increased solubility and anti-inflammatory activity compared to single piperine. Therefore, Pip-HBA multicomponent system has quite potential for further preparation development.

1. Introduction

Globally, in 2020 around 595 million people worldwide suffered from osteoarthritis which has increased by 132 % since 1990 [1]. Osteoarthritis (OA) is caused by joint fluid deficiency and causes inflammation [2,3]. Inflammation is usually mediated by inflammatory mediators such as cyclooxygenase, cytokines, adipokines, chemokines, and several matrix metalloproteinases [4–6]. OA causes symptoms such as pain, changes in joint shape, and impaired movement. Many drugs are used to treat OA, one of which is anti-inflammatory agents like non-steroidal anti-inflammatory drugs (NSAIDs) [7,8]. NSAIDs can treat inflammatory diseases due to the body's response to all stimuli [9–13]. On the other hand, if NSAIDs are used continuously over a long period, they will cause health

* Corresponding author.

E-mail address: ilma_nugrahani@itb.ac.id (Ilma Nugrahani).

<https://doi.org/10.1016/j.heliyon.2024.e31548>

Received 3 December 2023; Received in revised form 16 May 2024; Accepted 17 May 2024

Available online 23 May 2024

2405-8440/© 2024 Published by Elsevier Ltd.

This is an open access article under the CC BY-NC-ND license

(<http://creativecommons.org/licenses/by-nc-nd/4.0/>).

problems such as gastrointestinal irritation, kidney problems, cardiovascular risk, and liver disorder [14–17]. Besides chemical drugs, various herbal medicines derived from plant metabolites have been used to treat this disease, including piperine [18,19].

Piperine is the major compound in the Piperaceae plant, belonging to the group of alkaloid secondary metabolites [20]. Some research showed that piperine has many pharmacological effects such as anti-inflammatory, anti-osteoarthritis, anti-rheumatoid arthritis, and anti-cancer [21–24]. On the other hand, piperine has very low solubility in water, only about 40 mg/L [25]. Low solubility results in low absorption and bioavailability of piperine, so its pharmacological effects will also be reduced [26]. One of the efforts to develop drugs or nutraceuticals is the creation of multicomponent system [27].

Several studies have succeeded in developing piperine multicomponent system including piperine-succinic acid, piperine-saccharin, and resveratrol-piperine [28–30]. The piperine-succinic acid combination compound can improve the solubility of piperine up to 4 times [28]. The formation of the multicomponent system may involve non-covalent bonds (ionic bonds and non-ionic bonds) [31]. Ionic bonds produce salt, while non-ionic bonds produce neutral compounds or cocrystal [32,33]. Cocrystals consist of active pharmaceutical ingredients (API) and counter ions which form non-covalent interactions [34–37]. For a compound to form a multicomponent system, it must have a bonding site or synthon that is responsible for the compound interaction [38]. The piperine compound, a weak base (pKa 12.22), can interact with an acid compound [39]. Organic acid compounds such as hydroxybenzoic acid (HBA), a weak acid (pKa = 4.54), can potentially form multicomponent system with piperine [40]. Fig. 1 below show the structures of piperine (a) and 4-hydroxybenzoic acid (b).

HBA has a higher solubility in water than piperine, namely 5000 mg/L. Beside that HBA also has an anti-inflammatory effect so it is hoped that the resulting multicomponent system of piperine with hydroxybenzoic acid will increase the solubility of piperine and its anti-inflammatory/anti-osteoarthritis effect [42].

2. Materials and methods

2.1. Materials

The study used piperine >95 % (Synaptent LLC, Chicago, USA); 4-hydroxybenzoic acid >99 % (Tokyo Chemical Industry, Tokyo, Japan); KBr (Merck, Jakarta, Indonesia); 95 % ethanol and distilled water (Sakura Medical, Bandung, Indonesia); aluminum plate and cover (Rigaku, Tokyo, Japan); and capillary tube (CV. Prima Medica, Bandung, Indonesia).

2.2. Methods

2.2.1. Molar ratio screening

Molar ratio screening was carried out by mixing piperine-HBA with 1:1, 1:2, and 2:1 M ratios. A digital balance (Fujitsu FSR-A220, Tokyo, Japan) was used for sample weighing. Each mixture was crushed with a few drops of ethanol 95 % for 15 min until dry. Then the mixtures were measured for their melting range using electrothermal (Electrothermal AZ 9003, Staffordshire, UK). The appropriate mole ratio is the one that shows the new melting temperature most sharply.

2.2.2. Pip-HBA multicomponent system

The multicomponent system was made using solvent-dropped grinding (SDG). 95 % ethanol was dropped on the piperine-HBA 1:2 mixture until wet, then crushed for 15 min until dry, repeated the treatment 3 times. The slow evaporation method was used to obtain a single crystal for Single Crystal X-ray Diffraction (SCXRD). Pip-HBA 1:2 mixture was added 95 % ethanol, mixed until dissolved and transparent. The solution was placed in an Erlenmeyer and then allowed to evaporate at room temperature. The multicomponent system was characterized using an electrothermal analyzer, Differential Scanning Calorimeter, and Powder X-ray Diffractometer. Analysis using FTIR to confirm the existence of interactions between compounds. A selected single crystal was used for single-crystal X-ray Diffractometry (SCXRD) measurement.

2.2.3. Solid characterization and structure determination

Observation of the piperine, HBA, and Pip-HBA crystals were assisted using a binocular microscope (Olympus CX21, Tokyo, Japan). Thermal profile measurement used an electrothermal analyzer (Electrothermal AZ 9003, Staffordshire, UK) and DSC (Rigaku Thermoplus EVO2 DSC8231, Tokyo, Japan). PXRD Rigaku Miniflex (Tokyo, Japan) was used to analyze the multicomponent system.

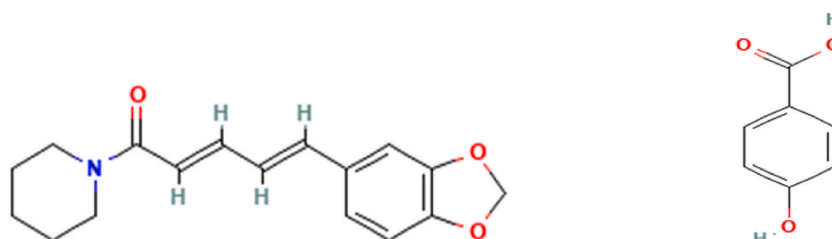


Fig. 1. The structure of (a) Piperine (Pip) and (b) 4-hydroxybenzoic acid (HBA) [40,41].

Analysis of the structure or interaction changes used FTIR Jasco 4200 Type-A (Oklahoma City, OK, USA). Three-dimensional structure determination using SCXRD XtaLAB Synergy-DW, Rigaku OD (Tokyo, Japan).

2.2.3.1. Optical observation of multicomponent system forms. Pip, HBA, and Pip-HBA crystals resulting from slow evaporation were put on an objective glass and were observed under a binocular microscope without a cover glass with 10× magnification. The pictures were taken by OPPO A3s cellular phone camera.

2.2.3.2. Electrothermal melt range measurement. About 1 mg of the sample was filled into a capillary tube with a hole in one end. The capillary tube was inserted into the sample holder, and the changes in the thermal profile were observed until it melted completely. Measurements started at a temperature of 30 °C with a heating rate at 10 °C/min [43].

2.2.3.3. Differential scanning calorimetry (DSC) analysis. About 1–3 mg of samples were crushed until smooth and inserted in an aluminum pan. Then, it was covered and packaged using a pressing tool. As a reference, an empty pan was placed next to the sample pan. The measurements were set at a temperature range of 30 °C–250 °C, and the heating rate at 10 °C/min [44].

2.2.3.4. Powder X-ray diffractometry (PXRD) analysis. About 100 mg samples were filled in a PXRD sample holder. Measurements were carried out at 2θ 3–60° intervals and a scanning speed of 0.01–3°/min, using Cu-Kα radiation with a graphite monochromator. Instrument current and voltage were set at 35 mA and 40 kV [45].

2.2.3.5. Fourier transform infrared (FTIR) analysis. The sample and KBr were mixed in a ratio of 1:100 until homogeneous, then put into a plate and pressed. The measurements were set at a wavenumber of 4000–400 cm⁻¹ [46].

2.2.3.6. Single crystal X-ray diffractometry (SCXRD) analysis. Suitable single crystals from the slow evaporation method were selected using a microscope. The selected single crystal is inserted into the SCXRD sample holder. Data were collected in ω-scan mode with a rotating anode source of Cu Kα radiation (λ = 1.54184 Å), X-ray optics at a temperature of –180 °C. CrysAlisPro software (Rigaku, Tokyo, Japan) was used to integrate the data. The crystal structure was solved directly with SHELXT, and refined with SHELXL [47,48]. The structure graph was prepared using the Mercury 4.3.1 program [49].

2.2.4. Solubility study

Pip-HBA multicomponent system, Pip, and HBA were dissolved in 100 mL distilled water. The samples were stirred using an orbital shaker, and more samples were added until the solutions were saturated. The sample concentrations in the solutions were determined using the derivative UV–Vis spectrophotometry method [28].

2.2.5. Anti-inflammatory activity

Ethical commission approval (No. 220/KEPK-Unisba/XI/2023, approved in Bandung, November 17, 2023) has been received for this anti-inflammatory study.

2.2.5.1. Animals. These experiments used male Wistar rats *Rattus norvegicus* (150–200 g) and were carried out following the regulations of the Institutional Animal Ethics Committee. The animals were placed in cages and provided with sufficient food and water.

2.2.5.2. Carrageenan-induced paw inflammation. Wistar rats *Rattus norvegicus* were divided into 7 groups (: Na-CMC (negative control), diclofenac sodium 4,5 mg/KgBW (standard drug), piperine 50 mg/kgBW, HBA 50 mg/kgBW, Pip-HBA 31 mg/KgBW (Pip-HBA 1), Pip-HBA 62 mg/KgBW (Pip-HBA 2), and Pip-HBA 125 mg/KgBW (Pip-HBA 3).

Edema was induced by sub-plantar induction of Carrageenan (0,1 mL of 1 % solution in 0,9 % saline solution) into the left hind paw 30 min after oral administration. Paw was measured after 30, 60, 120, 180, 240, 300, and 360 min of carrageenan induction by using a plethysmometer. The degree of inflammation is the difference between initial edema and after treatment.

Inflammation Percentage = $((V_t - V_o) / V_o) \times 100$.

V_t = paw volume at time t (after carrageenan induction)

V_o = initial paw volume (before carrageenan induction) [21].

2.3. Statistics

The data were presented as average values. Microsoft Excel (Microsoft Corp., Redmond, WA, USA) was used to create the curves. The anti-inflammatory data were processed using one-way ANOVA and Tukey's test.

3. Results and discussions

3.1. Molar ratio screening

Molar ratio screening by testing the melting range of 3-M ratios, namely 1:2, 1:1, and 2:1. The research results showed that a 1:2

mol ratio has the sharpest melting temperature. This showed that a molar ratio of 1:2 is the combination with the most suitable stoichiometric ratio. Molar ratio screening is shown in Table 1.

3.2. Pip-HBA preparation and characterization

Pip-HBA multicomponent system was obtained from SDG and solvent evaporation with a 1:2 M ratio produced yellowish powders and crystals. Fig. 2 below shows the single-crystal appearance of piperine (a), HBA (b), and Pip-HBA under 10× magnification.

Observation under a microscope showed that the Pip-HBA crystal's shape was different from the starting material. Pip-HBA was radiating-shaped, while piperine was blade-shaped, and HBA was branch-shaped.

The DSC thermogram also showed differences in thermal profiles. The pip-HBA multicomponent system melted at 121 °C with a sharper endothermic peak, while its physical mixture melted at 95 °C with a wider endothermic peak. This showed that the Pip-HBA multicomponent system formed a new solid phase, while the physical mixture was not new. Furthermore, the Pip-HBA multicomponent system degraded at 180 °C, while the PM at 175 °C, confirmed by electrothermal observation, showed a brown color. Thermogram profiles are shown in Fig. 3.

Next, to determine the formation of a new phase, measurements will be carried out using PXRD. The diffractogram of Pip-HBA multicomponent system and constituent materials are displayed in Fig. 4.

Changes in the diffractogram profile were seen by the appearance compounds peak at $2\theta = 7,82^\circ; 11,37^\circ; 15,66^\circ; 17,05^\circ; 20,74^\circ; 24,68^\circ; 25,43^\circ; \text{ dan } 30,84^\circ$ which is different from Pip and HBA. This showed that a new phase has formed.

Next, to analyze intermolecular interactions in the new structure, FTIR measurements were carried out (Fig. 5). This figure showed the change in the Pip-HBA spectrum compared to PM and the starting material, which occurred in the OH group from 3374 cm^{-1} to 3278 cm^{-1} , and the C=O group from 1677 cm^{-1} to 1681 cm^{-1} .

3.3. Structural study

3D structure determination was carried out using SCXRD. The Figures below are a thermal ellipsoid plot (Fig. 6) and a packing diagram of Pip-HBA (Fig. 7).

Two HBA molecules are forming double hydrogen bonds with COOH dimer motif. An OH group hydrogen bonded to the O=C group of piperine (Fig. 6). In the multi-component structure in three dimensions, the HBA dimers were connected by OH...O hydrogen bonds forming a chain structure along $[-1\ 1\ 0]$ direction. Piperine molecules attached to the ribbon via OH...O=C (pip) hydrogen bonds, thus two rows ribbon structure parallel to $(-1\ 1\ 0)$ plane was constructed as the unit structure of this multi-component crystal (Fig. 7(a)). This ribbon structure does not have further hydrogen bonds with other molecules. The ribbon structures were bundled into parallel and antiparallel (related by symmetry centers) to form layered crystal structures (Fig. 7(b), (c)). Table 2 below is the Pip-HBA crystallographic data, and the related CIF file and CheckCIF have been included in the supplementary material.

3.4. Solubility data

In determining solubility, data was obtained that the solubility of piperine in the Pip-HBA cocrystal increased compared with the solubility of single piperine, as shown in Table 3, and Fig. 8 below.

The solubility increase of piperine in Pip-HBA was 3-fold and significantly different ($P < 0.05$) from single piperine (Fig. 8(a)). Increasing solubility can be influenced by changes in the thermodynamics of the solid phase [50]. Another factor is the more soluble coformer molecules. HBA molecules will dissolve from the cocrystal and leave an empty channel structure, then the stability of the cocrystal becomes low. It is also discussed that layered crystal structure increases crystal solubility [51]. Regarding the interaction between piperine and HBA in crystals, the HBA dimer tends to stack easily on top of piperine molecules, resulting in an alternating layered structure. This stacking behavior of HBA prevents the formation of a strong piperine stacking structure, as observed in single piperine crystals. Consequently, the interaction of piperine molecules weakens in Pip-HBA, which leads to increased solubility. However, the solubility of HBA in Pip-HBA multicomponent was much lower and significantly different ($P < 0.05$) from the solubility of single HBA (Fig. 8(b)).

3.5. Anti-inflammatory Activities

The anti-inflammatory activity is the ability of the compound/agent to reduce or suppress the degree of edema produced by inducers in animal tests [52]. The inflammatory inducer used carrageenan, which can stimulate the production of bradykinin, histamine, tachykinin, reactive oxygen, and nitrogen species as inflammatory and pro-inflammatory mediators. Symptoms of inflammation like

Table 1
Molar ratio screening.

No.	Molar Ratio	Melting point (°C)
1.	1:2	90–95
2.	1:1	107–120
3.	2:1	105–119



(a) (b) (c)

Fig. 2. Crystals form (a) Piperine (b) HBA, and (c) Pip-HBA under 10× magnification.

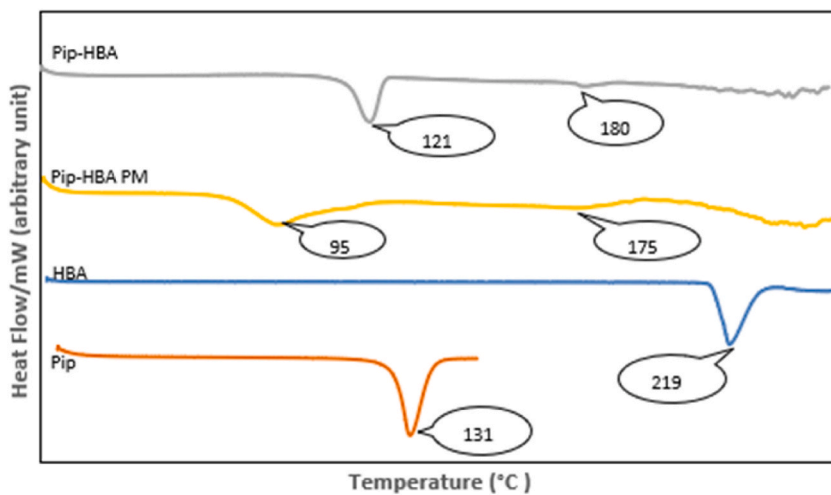


Fig. 3. DSC thermogram of Pip-HBA multicomponent system compared to its constituent components (Pip and HBA), and physical mixture (Pip-HBA PM)

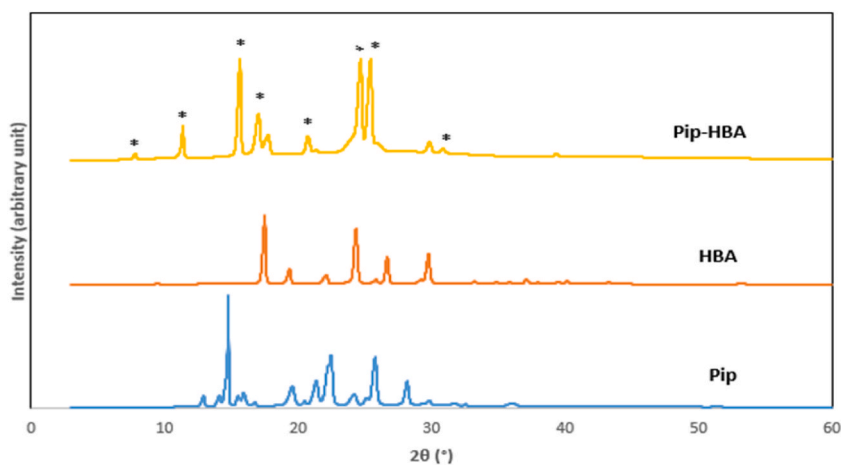


Fig. 4. Pip-HBA diffractogram compared to the constituent compounds (Piperine and HBA).

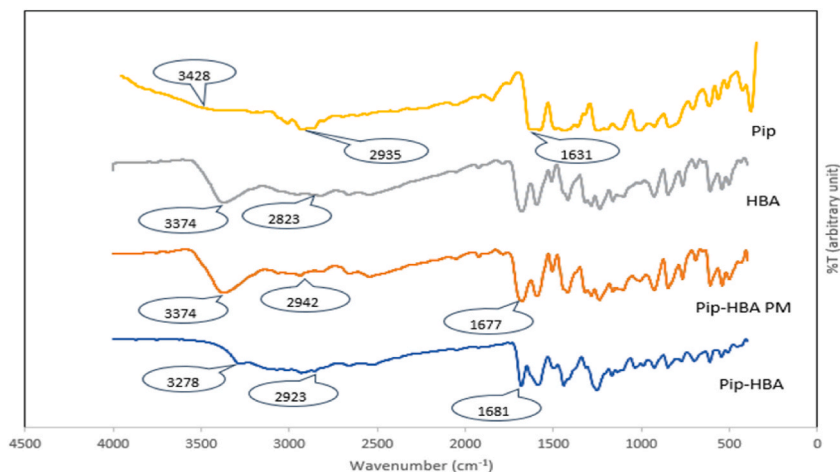


Fig. 5. FTIR spectra of Pip-HBA compared to piperine, HBA, and its PM

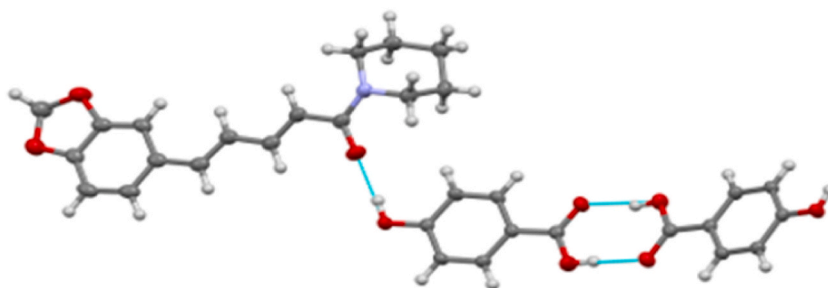


Fig. 6. Thermal ellipsoid plot of Pip-HBA cocrystal with 50 % probability. Hydrogen bonds were shown as blue lines. (For interpretation of the references to color in this figure legend, the reader is referred to the Web version of this article.)

edema, hyperalgesia, and erythema, which develop soon after carrageenan induction [53]. The following is the inflammatory response presented in the percentage of inflammation in Fig. 9 and Table 4.

Anti-inflammatory tests are shown in Fig. 9 and Table 4 which illustrates that Pip-HBA showed better anti-inflammation than single Pip and HBA. All data were checked with One-Way ANOVA showing significant differences in responses ($P < 0.05$), then followed by the Tukey test. Based on Table 4 administration of the Pip-HBA can begin to inhibit inflammation at 30 min after administration of carrageenan. At 60, 120, 180, 240, 300, and 360 min the anti-inflammatory activity of Pip-HBA was significantly different from single pip and HBA. At 300 min and 360 min, the anti-inflammatory activity of Pip-HBA dose 3 was not significantly different from diclofenac (grouping information using the Tukey method with 95 % confidence level). The increase in anti-inflammatory activity of the Pip-HBA multicomponent system was thought to be caused by increasing the solubility of piperine in the combination. Increasing solubility will result in a faster dissolution rate which has an impact on increasing bioavailability. On the other hand, the solubility of HBA in combination decreases compared to single HBA, which can result in increased permeability thereby increasing its absorptivity in the body.

4. Conclusions

We combined two natural ingredients, anti-inflammatories, piperine (Pip) and 4-hydroxybenzoic acid (HBA). The Pip-HBA multicomponent system has been successfully prepared, characterized, and structure determined. They were then tested for solubility and anti-inflammatory activity. According to a solubility test, the Pip-HBA was more soluble in water than single piperine. Furthermore, the Pip-HBA has better anti-inflammation activity than single piperine.

Ethics statement: The animal study was approved by Health Research Ethics Committee, Bandung Islamic University with the approval number: 220/KEPK-Unisba/XI/2023.

Data availability statement

Data included in article/supp. material/referenced in the article. The crystal structure has been deposited in CCDC (Cambridge Crystallography Data Center) number 2298890. CCDC 2298890 contains the supplementary crystallographic data for this paper. The

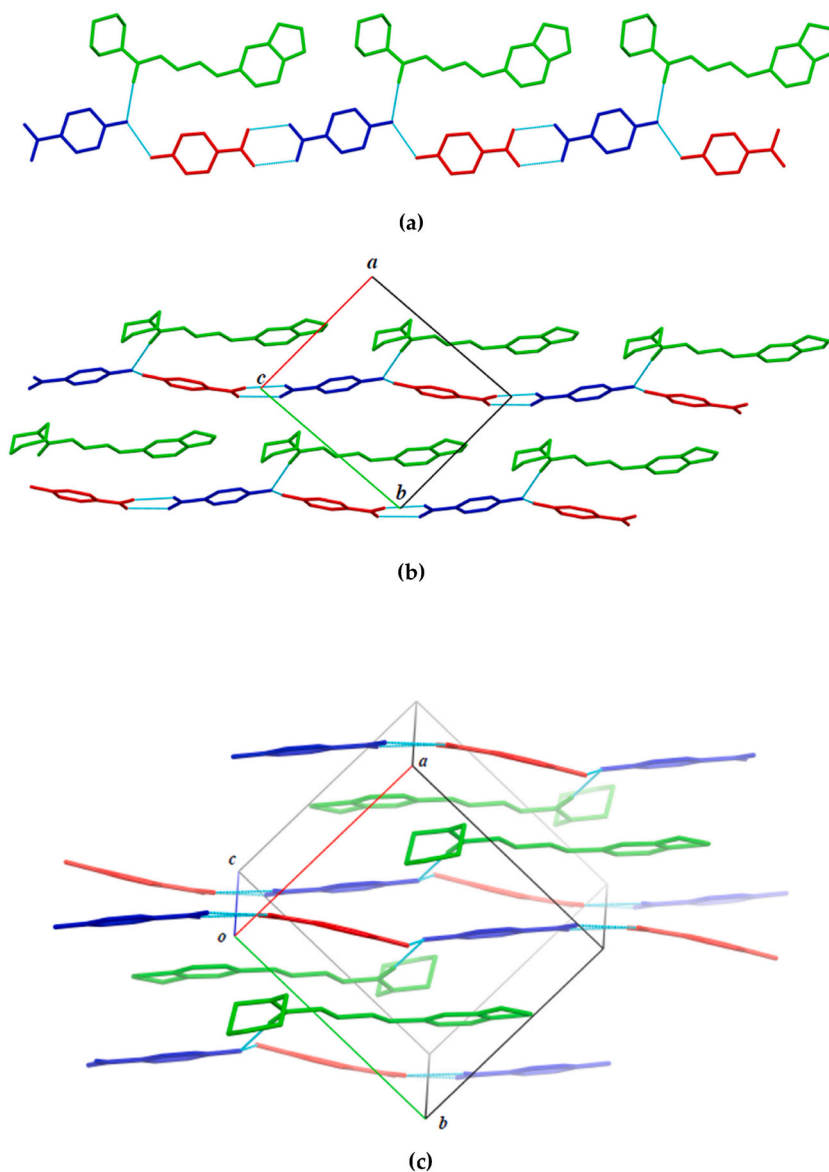


Fig. 7. Packing diagrams of Pip-HBA (green: piperine; red & blue: HBA). The light blue color represents hydrogen bonds. (a) Pip-HBA ribbon structure, (b) Parallel part of Pip-HBA ribbon viewed along c-axis, (c) Pip-HBA layered structure. (For interpretation of the references to color in this figure legend, the reader is referred to the Web version of this article.)

data can be obtained free of charge from The Cambridge Crystallographic Data Centre via www.ccdc.cam.ac.uk/structures.

Funding statement

This work was supported by Hibah Riset Unggulan Pusat dan Pusat Penelitian (RU3P) 2023 (Contract number 487L/IT1.A/SK-KP/2023) managed by The Institute for Science and Technology Development (LPIT), Bandung Institute of Technology. Part of this work was supported by JSPS KAKENHI Grant Number JP20H04661 and JP22K05032 (HU).

CRediT authorship contribution statement

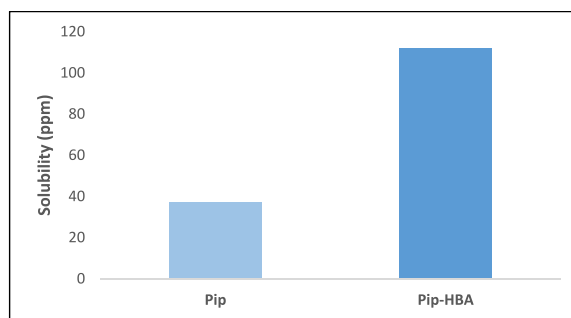
Ari Sartinah: Writing – review & editing, Writing – original draft, Project administration, Methodology, Investigation, Formal analysis, Data curation, Conceptualization. **Hidehiro Uekusa:** Writing – review & editing, Software, Resources, Methodology, Data curation, Conceptualization. **Yuto Abekura:** Methodology, Investigation, Formal analysis, Data curation. **Slamet Ibrahim:** Supervision, Methodology. **Kusnandar Anggadiredja:** Supervision, Methodology. **Ilma Nugrahani:** Writing – review & editing, Writing –

Table 2
Crystal data for Pip-HBA.

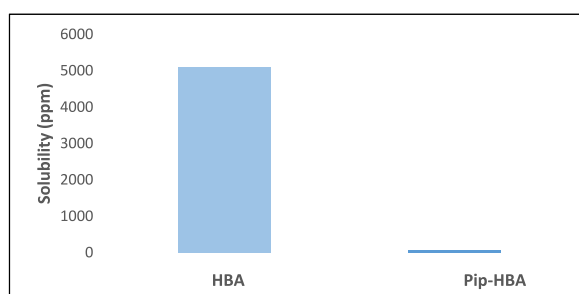
Parameters	Pip-HBA	
Compound Name	Piperine 4-Hydroxybenzoate	
Empirical formula	C ₃₁ H ₃₁ N O ₉	
Formula weight	561.57	
Temperature	93 (2) K	
Wavelength	1.54184 Å	
Crystal system	Triclinic	
Space group	P $\bar{1}$	
Unit cell dimensions	a = 10.6351 (2) Å b = 11.3170 (2) Å c = 12.3229 (3) Å	$\alpha = 84.659 (2)^\circ$ $\beta = 65.382 (2)^\circ$ $\gamma = 84.008 (2)^\circ$
Volume	1338.96 (5) Å ³	
Z	2	
Density (calculated)	1.393 g/cm ³	
Absorption coefficient	0.854 mm ⁻¹	
F (000)	592	
Crystal size	0.310 x 0.220 x 0.210 mm ³	
Theta range for data collection	3.933–74.552°	
Reflections collected	14651	
Independent reflections	5255 [R (int) = 0.0379]	
Goodness-of-fit on F ²	1.037	
Final R indices [I > 2sigma(I)]	R1 = 0.0409, wR2 = 0.1058	
R indices (all data)	R1 = 0.0496, wR2 = 0.1102	
CCDC Deposit Number	2298890	

Table 3
Solubility of piperine in Pip-HBA and single piperine (Pip); HBA in Pip-HBA and single HBA.

No.	Samples	Solubility (mean \pm RSD ppm)
1.	Single Pip	37.46 \pm 1.70
2.	Pip in Pip-HBA	112.5 \pm 0.84
3.	Single HBA	5102.79 \pm 0.019
4.	HBA in Pip-HBA	64.2 \pm 0.015



(a)



(b)

Fig. 8. Solubility of (a) piperine in Pip-HBA and single piperine (Pip), (b) HBA in Pip-HBA and single HBA; (n = 3); RSD \leq 2; P < 0.05

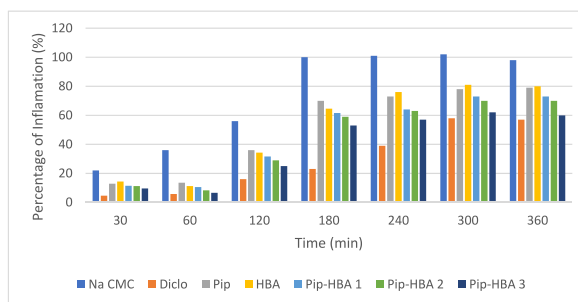


Fig. 9. Percentage of inflammation of Na CMC, diclofenac sodium (diclo), piperine (Pip), 4-hydroxybenzoic acid (HBA), and Pip-HBA (three dosage variations) on carrageenan-induced inflammation.

Table 4

Percentage of inflammation of Na CMC, diclofenac sodium (diclo), piperine (Pip), 4-hydroxybenzoic acid (HBA), and Pip-HBA (three dosage variations) on carrageenan-induced inflammation.

Samples	Percentage of Inflammation (mean \pm SD %)						
	T1/2	T1	T2	T3	T4	T5	T6
Na CMC	22.113 \pm 0.650	36.00 \pm 3.61	56.00 \pm 1.73	99.00 \pm 1.73	101.00 \pm 1.73	102.667 \pm 0.577	101.000 \pm 1.000
Pip	12.967 \pm 1.079	13.67 \pm 2.89	36.00 \pm 3.00	70.333 \pm 1.155	73.667 \pm 1.528	78.67 \pm 2.08	70.333 \pm 1.155
HBA	14.437 \pm 0.649	11.333 \pm 0.577	34.33 \pm 4.16	64.667 \pm 1.528	76.667 \pm 1.528	81.667 \pm 1.155	64.667 \pm 1.528
Pip-HBA 1	11.483 \pm 1.068	10.667 \pm 1.155	31.67 \pm 3.51	61.67 \pm 2.08	64.33 \pm 2.52	73.333 \pm 1.155	61.67 \pm 2.08
Pip-HBA 2	11.370 \pm 1.025	8.333 \pm 0.577	29.333 \pm 1.155	59.000 \pm 1.000	63.333 \pm 1.528	70.00 \pm 1.73	59.000 \pm 1.000
Pip-HBA 3	9.660 \pm 0.758	6.617 \pm 0.861	25.333 \pm 1.155	51.000 \pm 1.000	57.667 \pm 1.155	62.67 \pm 2.52	51.000 \pm 1.000
Diclo	3.125 \pm 0.000	5.833 \pm 0.722	16.00 \pm 1.73	23.33 \pm 4.04	39.667 \pm 0.577	58.67 \pm 3.51	57.67 \pm 2.52

original draft, Supervision, Resources, Methodology, Formal analysis, Data curation, Conceptualization.

Declaration of competing interest

The authors declare the following financial interests/personal relationships which may be considered as potential competing interests:

Hidehiro Uekusa reports financial support was provided by JSPS KAKENHI. If there are other authors, they declare that they have no known competing financial interests or personal relationships that could have appeared to influence the work reported in this paper.

Abbreviations

DSC	Differential Scanning Calorimetry
FTIR	Fourier Transform Infrared
HBA	4-Hydroxybenzoic acid
KgBW	ilogram Body Weight
NMR	Nuclear Magnetic Resonance
OA	Osteoarthritis
Pip	Piperine
PXRD	Powder X-Ray Diffractometry
SCXRD	Single Crystal X-Ray Diffractometry

References

- [1] J.D. Steinmetz, G.T. Culbreth, L.M. Haile, Q. Rafferty, J. Lo, K.G. Fukutaki, J.A. Cruz, A.E. Smith, S.E. Vollset, P.M. Brooks, M. Cross, Global, regional, and national burden of osteoarthritis, 1990–2020 and projections to 2050: a systematic analysis for the Global Burden of Disease Study 2021, *The Lancet Rheumatology* 5 (9) (2023) e508–e522.
- [2] S. Zhu, J. Zhu, G. Zhen, Y. Hu, S. An, Y. Li, X. Cao, Subchondral bone osteoclasts induce sensory innervation and osteoarthritis pain, *J. Clin. Investig.* 129 (3) (2019) 1076–1093.
- [3] B. Xia, D. Chen, J. Zhang, S. Hu, H. Jin, P. Tong, Osteoarthritis pathogenesis: a review of molecular mechanisms, *Calcif. Tissue Int.* 95 (6) (2014) 495–505.
- [4] V. Molnar, V. Matišić, I. Kodvanj, R. Bjelica, Ž. Jeleč, D. Hudetz, D. Primorac, Cytokines and chemokines involved in osteoarthritis pathogenesis, *Int. J. Mol. Sci.* 22 (17) (2021) 9208.

- [5] X. Houard, M.B. Goldring, F. Berenbaum, Homeostatic mechanisms in articular cartilage and role of inflammation in osteoarthritis, *Curr. Rheumatol. Rep.* 15 (2013) 1–10.
- [6] Y.Y. Chow, K.Y. Chin, The role of inflammation in the pathogenesis of osteoarthritis, *Mediat. Inflamm.* 2020 (2020).
- [7] B.R. da Costa, S. Reichenbach, N. Keller, L. Nartey, S. Wandel, P. Jüni, S. Trelle, Effectiveness of non-steroidal anti-inflammatory drugs for the treatment of pain in knee and hip osteoarthritis: a network meta-analysis, *Lancet* 390 (10090) (2017) e21–e33.
- [8] A. Magni, P. Agostoni, C. Bonezzi, G. Massazza, P. Menè, V. Savarino, D. Fornasari, Management of osteoarthritis: expert opinion on NSAIDs, *Pain and Therapy* (2021) 1–26.
- [9] D. Laveti, M. Kumar, R. Hemalatha, R. Sistla, V. Gm Naidu, V. Talla, R. Nagpal, Anti-inflammatory treatments for chronic diseases: a review, *Inflammation & Allergy-Drug Targets (Formerly Current Drug Targets-Inflammation & Allergy)(Discontinued)* 12 (5) (2013) 349–361.
- [10] L. Chen, H. Deng, H. Cui, J. Fang, Z. Zuo, J. Deng, L. Zhao, Inflammatory responses and inflammation-associated diseases in organs, *Oncotarget* 9 (6) (2018) 7204.
- [11] G. Harvanová, S. Duranková, J. Bernasovská, The role of cytokines and chemokines in the inflammatory response, *Alergologia Polska-Polish Journal of Allergy* 10 (3) (2023) 210–219.
- [12] P.N. Madianos, Y.A. Bobetsis, D.F. Kinane, Generation of inflammatory stimuli: how bacteria set up inflammatory responses in the gingiva, *J. Clin. Periodontol.* 32 (2005) 57–71.
- [13] K.A. Ali, A. Maity, S.D. Roy, S.D. Pramanik, P.P. Das, M.A. Shaharyar, Insight into the mechanism of steroidal and non-steroidal anti-inflammatory drugs, in: *How Synthetic Drugs Work*, Academic Press, 2023, pp. 61–94.
- [14] S. Bindu, S. Mazumder, U. Bandyopadhyay, Non-steroidal anti-inflammatory drugs (NSAIDs) and organ damage: a current perspective, *Biochem. Pharmacol.* 180 (2020) 114147.
- [15] U.F. Kholmurodovich, Damage to the digestive system when using non-steroidal anti-inflammatory drugs, *European journal of modern medicine and practice* 2 (1) (2022) 6–16.
- [16] A. Cabassi, S. Tedeschi, S. Perlini, I. Verzicco, R. Volpi, G. Gonzi, S.D. Canale, Non-steroidal anti-inflammatory drug effects on renal and cardiovascular function: from physiology to clinical practice, *European journal of preventive cardiology* 27 (8) (2020) 850–867.
- [17] P. Sriuththa, B. Sirichanchuen, U. Permsuwan, Hepatotoxicity of nonsteroidal anti-inflammatory drugs: a systematic review of randomized controlled trials, *Bangladesh Liver J.* 2018 (2018).
- [18] X. Ying, X. Chen, S. Cheng, Y. Shen, L. Peng, H. zi Xu, Piperine inhibits IL- β induced expression of inflammatory mediators in human osteoarthritis chondrocyte, *Int. Immunopharm.* 17 (2) (2013) 293–299.
- [19] A.A. Faruqui, Curcumin and piperine: a novel therapy in the management of osteoarthritis in Indian patient, *Pacific Journal of Medical Sciences* 18 (1) (2018) 36–43.
- [20] A. Tiwari, K.R. Mahadik, S.Y. Gabhe, Piperine: a comprehensive review of methods of isolation, purification, and biological properties, *Medicine in Drug Discovery* 7 (2020) 100027.
- [21] N. Dhargawe, S. Mahalkalkar, B. Mohod, J.P. Raj, Evaluation of Analgesic, anti-inflammatory, and Antipyretic activity of piperine: an experimental study, *Pharmacogn. Res.* 12 (2) (2021).
- [22] R. Vaishya, A.K. Agarwal, A. Shah, V. Vijay, A. Vaish, Current status of top 10 nutraceuticals used for Knee Osteoarthritis in India, *J. Clin. Orthop. Trauma* 9 (4) (2018) 338–348.
- [23] V. Murunikkara, S.J. Pragasam, G. Kodandaraman, E.P. Sabina, M. Rasool, Anti-inflammatory effect of piperine in adjuvant-induced arthritic rats—a biochemical approach, *Inflammation* 35 (2012) 1348–1356.
- [24] A. Manayi, S.M. Nabavi, W.N. Setzer, S. Safari, Piperine as a potential anti-cancer agent: a review on preclinical studies, *Curr. Med. Chem.* 25 (37) (2018) 4918–4928.
- [25] L. Gorgani, M. Mohammadi, G.D. Najafpour, M. Nikzad, Piperine—the bioactive compound of black pepper: from isolation to medicinal formulations, *Compr. Rev. Food Sci. Food Saf.* 16 (1) (2017) 124–140.
- [26] H.U. Salsabila, L.I. Fitriani, E.R. Zaini, Recent strategies for improving solubility and oral bioavailability of piperine, *Int. J. Appl. Pharm.* 13 (4) (2021) 31–39.
- [27] I. Nugrahani, R.D. Parwati, Challenges and progress in nonsteroidal anti-inflammatory drugs co-crystal development, *Molecules* 26 (14) (2021) 4185.
- [28] E.Afriyani Zaini, L. Fitriani, F. Ismed, A. Horikawa, H. Uekusa, Improved solubility and dissolution rates in novel multicomponent system crystals of piperine with succinic acid, *Sci. Pharm.* 88 (2) (2020) 21.
- [29] E. Zaini, D. Riska, M.D. Oktavia, F. Ismed, L. Fitriani, Improving Dissolution rate of piperine by multicomponent system crystal formation with saccharin, *Res. J. Pharm. Technol.* 13 (4) (2020) 1928–1932.
- [30] H. He, Q. Zhang, J.R. Wang, X. Mei, Structure, physicochemical properties and pharmacokinetics of resveratrol and piperine cocrystals, *CrystEngComm* 19 (41) (2017) 6154–6163.
- [31] I. Nugrahani, D. Herawati, M.S. Wibowo, The benefits and challenges of antibiotics–non-steroidal anti-inflammatory drugs non-covalent reaction, *Molecules* 28 (9) (2023) 3672.
- [32] D.J. Berry, J.W. Steed, Pharmaceutical cocrystals, salts and multicomponent system systems; intermolecular interactions and property based design, *Adv. Drug Deliv. Rev.* 117 (2017) 3–24.
- [33] I. Nugrahani, M.A. Jessica, Amino acids as the potential co-former for co-crystal development: a review, *Molecules* 26 (11) (2021) 3279.
- [34] I. Nugrahani, R.D. Parwati, Challenges and progress in nonsteroidal anti-inflammatory drugs co-crystal development, *Molecules* 26 (14) (2021) 4185.
- [35] D. Ejarque, T. Calvet, M. Font-Bardia, J. Pons, Cocrystals based on 4, 4'-bipyridine: influence of crystal packing on melting point, *Crystals* 11 (2) (2021) 191.
- [36] F. Sánchez-Férez, D. Ejarque, T. Calvet, M. Font-Bardia, J. Pons, Isonicotinamide-based compounds: from cocrystal to polymer, *Molecules* 24 (22) (2019) 4169.
- [37] D. Ejarque, T. Calvet, M. Font-Bardia, J. Pons, Virtual assessment achieved two binary cocrystals based on a liquid and a solid pyridine derivative with modulated thermal stabilities, *CrystEngComm* 25 (34) (2023) 4798–4811.
- [38] L. Wang, L. Zhao, M. Liu, R. Chen, Y. Yang, Y. Gu, Multi-component hydrogen-bonding salts formed between imidazole and aromatic acids: synthons cooperation and crystal structures, *Sci. China Chem.* 55 (2012) 2115–2122.
- [39] A.K. Nugroho, N. Kusumorini, S. Pramono, R. Martien, An update on nanoparticle formulation design of piperine to improve its oral bioavailability: a review, *Iraqi Journal of Pharmaceutical Sciences* 32 (1) (2023) 14–30 (P-ISSN 1683-3597 E-ISSN 2521-3512).
- [40] National Center for Biotechnology Information. PubChem compound summary for 4-hydroxybenzoic acid. Available online: <https://pubchem.ncbi.nlm.nih.gov/compound/135> (accessed on 20 September 2023)[Not Available in CrossRef][Not Available in].
- [41] National Center for Biotechnology Information. PubChem compound summary for piperine. Available online: <https://pubchem.ncbi.nlm.nih.gov/compound/Piperine> (accessed on 20 September 2023)[].
- [42] A.N. Winter, M.C. Brenner, N. Punessen, M. Snodgrass, C. Byars, Y. Arora, D.A. Linseman, Comparison of the neuroprotective and anti-inflammatory effects of the anthocyanin metabolites, protocatechuic acid and 4-hydroxybenzoic acid, *Oxid. Med. Cell. Longev.* 2017 (2017).
- [43] I. Nugrahani, A.N. Laksana, H. Uekusa, H. Oyama, New organic salt from levofloxacin-citric acid: what is the impact on the stability and antibiotic potency? *Molecules* 27 (7) (2022) 2166. Ugn.
- [44] M. Abd-Elghany, T.M. Klapötke, A review on differential scanning calorimetry technique and its importance in the field of energetic materials, *Physical Sciences Reviews* 3 (4) (2018) 20170103.
- [45] I. Nugrahani, D. Utami, S. Ibrahim, Y.P. Nugraha, H. Uekusa, Zwitterionic cocrystal of diclofenac and L-proline: structure determination, solubility, kinetics of cocrystallization, and stability study, *Eur. J. Pharmaceut. Sci.* 117 (2018) 168–176.
- [46] I. Nugrahani, S.W. Komara, A. Horikawa, H. Uekusa, Composing novel diclofenac potassium and l-proline salt cocrystal as a strategy to increase solubility and dissolution, *J. Pharmaceut. Sci.* 109 (11) (2020) 3423–3438.
- [47] G.M. Sheldrick, SHELXT—Integrated space-group and crystal-structure determination, *Acta Crystallogr. A: Foundations and Advances* 71 (1) (2015) 3–8.
- [48] G.M. Sheldrick, Crystal structure refinement with SHELXL, *Acta Crystallogr., Sect. C: Struct. Chem.* 71 (1) (2015) 3–8.

- [49] I. Nugrahani, R.A. Kumalasari, W.N. Auli, A. Horikawa, H. Uekusa, Salt cocrystal of diclofenac sodium-l-proline: structural, pseudopolymorphism, and pharmaceuticals performance study, *Pharmaceutics* 12 (7) (2020) 690.
- [50] E. Batisai, A. Ayamine, O.E. Kilinkissa, N.B. Báthori, Melting point–solubility–structure correlations in multicomponent system crystals containing fumaric or adipic acid, *CrystEngComm* 16 (43) (2014) 9992–9998.
- [51] O.D. Putra, D. Umeda, Y.P. Nugraha, T. Furuishi, H. Nagase, K. Fukuzawa, H. Uekusa, E. Yonemochi, Solubility improvement of epalrestat by layered structure formation via cocrystallization, *CrystEngComm* 19 (19) (2017) 2614–2622.
- [52] L. Ziyang, Z. Yongmei, Z. Nan, T. Ning, L. Baolin, Evaluation of the anti-inflammatory activity of luteolin in experimental animal models, *Planta Med.* 73 (3) (2007) 221–226.
- [53] S.F. Ahmad, S.M. Attia, S.A. Bakheet, K.M. Zoheir, M.A. Ansari, H.M. Korashy, A.R. Abd-Allah, Naringin attenuates the development of carrageenan-induced acute lung inflammation through inhibition of NF- κ B, STAT3 and pro-inflammatory mediators and enhancement of I κ B α and anti-inflammatory cytokines, *Inflammation* 38 (2015) 846–857.